Korean J. Chem. Eng., **27**(2), 459-464 (2010)
DOI: 10.1007/s11814-010-0086-x

Removal of sulfur dioxide from dibenzothiophene sulfone over Mg-based oxide catalysts prepared by spray pyrolysis

Young Kwon Park*, Sun Young Kim, Hyeon Joo Kim**, Kyeong Youl Jung**, Kwang-Eun Jeong***, Soon-Yong Jeong***, and Jong-Ki Jeon**,†**

*Faculty of Environmental Engineering, University of Seoul, Seoul 130-743, Korea
**Department of Chemical Engineering, Kongju National University, Gongju 314-701, Korea
***Petroleum Displacement Technology Research Center,
Korea Research Institute of Chemical Technology (KRICT), Daejeon 305-600, Korea
(*Received 25 June 2009 • accepted 4 September 2009*)

Abstract−Spray pyrolysis was used to prepare catalysts containing magnesium with mesopores. MgO-SiO_2, MgO-Al_2O_3, and MgO-SiO_2-Al_2O_3 catalysts were synthesized using cetyltrimethylammonium bromide (CTAB) as a templating agent. The characteristics of the catalysts were examined by N_2 adsorption, XRD, XRF and the temperature-programmed desorption of carbon dioxide. The MgO-SiO_2 catalyst has well-developed mesopores, a large surface area and well dispersed magnesium oxide. The basic sites on the MgO-SiO_2 catalyst were much stronger than those on the MgO-SiO_2-Al_2O_3 and MgO-Al_2O_3 catalysts. The catalytic performance for the decomposition of dibenzothiophene sulfone (DBTS) to biphenyl and sulfur dioxide gas was examined in a fixed-bed reactor. The MgO-SiO_2 catalyst has the highest activity in the cracking of DBTS, which was attributed to the strong basicity due to the dispersed effect of magnesium oxide. Compared to the MgO catalyst, the mesoporous MgO-SiO_2 solid base can improve significantly the catalytic efficiency for the removal of sulfur dioxide from dibenzothiophene sulfone.

Key words: Spray Pyrolysis, Dibenzothiophene Sulfone, Solid Base Catalyst, Desulfurization

INTRODUCTION

Since the research team of the Mobil Company published a study of mesoporous materials, various methods for manufacturing mesoporous particles arranged regularly have been attempted. Among them, the most widely used is the technique of self-assembly of a surfactant in the liquid phase [1,2]. The size and structure of pores can be controlled in a variety of ways depending on the types of surfactants as well as the types and features of templating agents. A wide range of functionalities can be imparted to mesoporous materials by producing them in particle, thin membrane, bar or fiber forms.

Traditionally, mesoporous materials have been synthesized by a liquid phase reaction based on a self-assembly technique [3-5]. After dissolving the high-molecular-weight templating agents in water or organic solvents or dispersing it, porous materials are synthesized by inducing self-assembly from solution directly with a precursor of the substances to be made. Although such methods can rapidly induce self-assembly, it is essential to allow a long time to secure a regular arrangement of pores within the particle.

Recently, the manufacture of sphere-type minute mesoporous particles using spray pyrolysis was reported [6-9]. In spray pyrolysis, a particle is formed from a single liquid droplet in a few seconds. Spray pyrolysis has been used to prepare multi-component functional inorganic particles [10-13]. The application of spray pyrolysis to the preparation of mesoporous materials has an advantage in that the processing time to achieve mesopores with regularity is a few seconds, which is much shorter than existing liquid phase methods. In addition, it can produce a spherical-shaped powder with a minute particle size and narrow particle size distribution [14]. Spray pyrolysis as an aerosol process has been successfully applied to synthesize ceramic particles with micron to submicron size. In spray pyrolysis, atomized liquid droplets lead to the formation of particles by evaporation, pyrolysis, and crystallization. So, the homogeneous mixing of all components in a droplet is achieved at nanometer scale. As a result, the prepared particles have relative uniformity in size, fine size and non-aggregation characteristics [15-17].

The current technologies for achieving low sulfur in diesel fuel are based on hydrotreating, which requires high temperatures, high pressures and an excessive supply of hydrogen. Oxidative desulfurization (ODS) is considered to be a promising new method for ultra deep desulfurization, which can be carried out under very mild conditions (atmospheric pressure, <100 °C) [18]. Dibenzothiophene sulfone (DBTS), which is one of the products of the oxidative desulfurization of heavy oil, can be removed by extraction and adsorption processes. However, it is necessary to utilize DBTS using catalytic cracking in order to prevent the loss of a useful fraction through extraction or adsorption. DBTS decomposes to biphenyl and sulfur dioxide gas.

Some major solid base catalysts include single component metal oxides, alkali metals supported on metal oxides, clay-type minerals, zeolites to which alkali metals are added or whose ions are exchanged [19-21]. The characteristics of zeolites are greatly affected by the types of positive ions exchanged or added. MgO, CaO, SrO and BaO, which are metal oxides in the family of alkali earth metals, are well known solid base catalysts [19]. It has been reported that

†To whom correspondence should be addressed.
E-mail: jkjeon@kongju.ac.kr

MgO demonstrates a high level of activity for the decomposition of DBTS [22].

The base-catalytic performance of Mg-Al mixed oxides has been reported to be related to the number of the basic sites, and that their basic sites are correlated strongly with the surface area [23]. In a previous study, it was reported that an Mg-Al-mesoporous silica catalyst formulated in a direct incorporation method showed higher catalytic performance during the catalytic removal of sulfur dioxide from DBTS than pure MgO [24].

In this study, spray pyrolysis was used to prepare catalysts containing magnesium with mesopores, such as MgO-SiO_2, MgO-Al_2O_3 and MgO-SiO_2-Al_2O_3 catalysts, using cetyltrimethylammonium bromide (CTAB) as a templating agent. The characteristics of the catalysts were examined by N_2 adsorption, XRD, XRF, and the temperature-programmed desorption of carbon dioxide. The catalytic performance during the decomposition of DBTS was examined in a fixed-bed reactor.

EXPERIMENTAL

1. Preparation of Catalysts

The following starting materials were used to produce complex oxides with mesopores via spray pyrolysis: tetraethyl orthosilicate (TEOS, Aldrich 98%) as a silica precursor; aluminum nitrate nonahydrate (Aldrich 98%) as a alumina precursor; magnesium nitrate hexahydrate (Aldrich, 99%) as a magnesium precursor; and cetyltrimethylammonium bromide (CTAB, Aldrich 99%) as a template. The method for manufacturing the complex oxide was as follows. CTAB was dissolved in distilled water at 35 °C. A metal precursor solution was prepared by dissolving magnesium nitrate hexahydrate and aluminum nitrate nonahydrate in distilled water. After the solutions were mixed, TEOS was added to make a clear spray solution.

The equipment for producing the catalyst by spray pyrolysis consisted of an ultrasonic droplet generator with 6 vibrators at 1.7 MHz (DongRim Co.), a quartz reactor (1,200 mm in length and 55 mm in external diameter) and a particle collector. The droplet produced by the generator was transferred by air to the quartz reactor for drying and thermal pyrolysis. The flow rate of compressed air was controlled to 10-40 *l*/min at room temperature. The reactor temperature in the drying and thermal-pyrolysis zones was kept at 50 °C and 450 °C, respectively, for smooth procedures, including the drying, extraction, pyrolysis and densification of the droplets produced by ultrasonic vibrators. The catalytic particles obtained through the final thermal-pyrolysis zone were collected with a porous Teflon filter. The catalyst produced was sintered at 550 °C for 4 hours to remove the remaining organic compounds.

In this study, three types of catalysts were synthesized by spray pyrolysis. MgAl is a catalyst made by spraying a solution containing the magnesium precursor, aluminum precursor and templating agent using spray pyrolysis. The magnesium oxide content in the catalyst after calcination was 52.4 wt% (Table 1). MgSiAl is a catalyst produced by spray pyrolysis of a solution of magnesium, aluminum and silicon precursors, and a templating agent. The weight percentage of MgO, SiO_2 and Al_2O_3 was 48.3, 17.7 and 34.0 wt%, respectively. MgSi was produced by spray pyrolysis of a solution of magnesium and a silicon precursor, and a templating agent. The magnesium oxide content in the catalyst after calcination was 53.4 wt%.

Table 1. Composition of catalysts synthesized by spray pyrolysis

Catalysts	Composition in catalysts (wt%)		
	MgO	SiO_2	Al_2O_3
MgAl	52.4	0	47.6
MgSiAl	48.3	34.0	17.7
MgSi	53.4	46.6	0.0

2. Characterization

The BET surface area of the catalyst was measured by using an ASAP 2010 apparatus by Micromeritics. A 0.3 g sample was taken after drying the catalyst. After outgassing for five hours at 250 °C in a vacuum, nitrogen was supplied as an adsorption gas at liquid nitrogen temperature, and the nitrogen adsorption-desorption isotherms and BET surface areas were obtained.

The morphology and the size of catalyst nanoparticles were observed by a high-resolution scanning electron microscope (HR-SEM, Tescan, MIRA LMH). The crystallinity of the catalysts was examined by XRD. The XRD patterns were obtained on a Rigaku D/MAX-II device with Cu Kα radiation energy. The Mg, Al and Si content in the catalyst was analyzed by fluorescence X-ray element analysis (XRF, Seiko Instruments, SEA 2220A).

Temperature-programmed desorption of CO_2 (CO_2-TPD) was used to analyze the basic sites of the catalysts [25]. CO_2-TPD was performed under a 20 ml/min argon flow at a heating rate of 10 °C/min. The catalysts were heated initially to 550 °C for 60 min in an argon flow. CO_2 was then absorbed at 50 °C for 30 min and the physically adsorbed CO_2 was removed under the same conditions. The effluent was analyzed with an on-line thermal conductivity detector.

3. Catalytic Activity

The DBTS decomposition reaction was performed in a fixed bed reactor. A 3 g sample of the catalyst was placed inside the reactor (Fig. 1). The internal pressure was controlled to 100 psi by using a back pressure regulator. The reaction temperature was 475 °C and the space velocity (WHSV) was 5 h^{-1}. Samples of the liquid product were collected at a constant interval and analyzed by XRF (XOS Sindie 7039XR).

RESULTS AND DISCUSSION

1. Characterization of Catalysts

Table 2 shows the BET surface area and pore volume of the catalyst obtained from the nitrogen adsorption/desorption experiment and Fig. 2 shows adsorption/desorption isotherm and pore size distribution. This shows that all the catalysts have adsorption/desorption-shaped mesopores, as shown in group IV. The BET surface areas were 131, 149 and 148 m^2/g in MgAl, MgSiAl and MgSi, respectively. Therefore, there were no large differences in the surface areas of the three catalysts prepared by spray pyrolysis. The pore volumes of all three catalysts were based on mesopores >1.7 nm in size. The pore volume was highest in MgSi followed by in turn MgSiAl and MgAl. As a result, MgSi, which was composed of magnesium oxide and silica, had the most well-developed mesopore structure as well as the largest pore size and surface area.

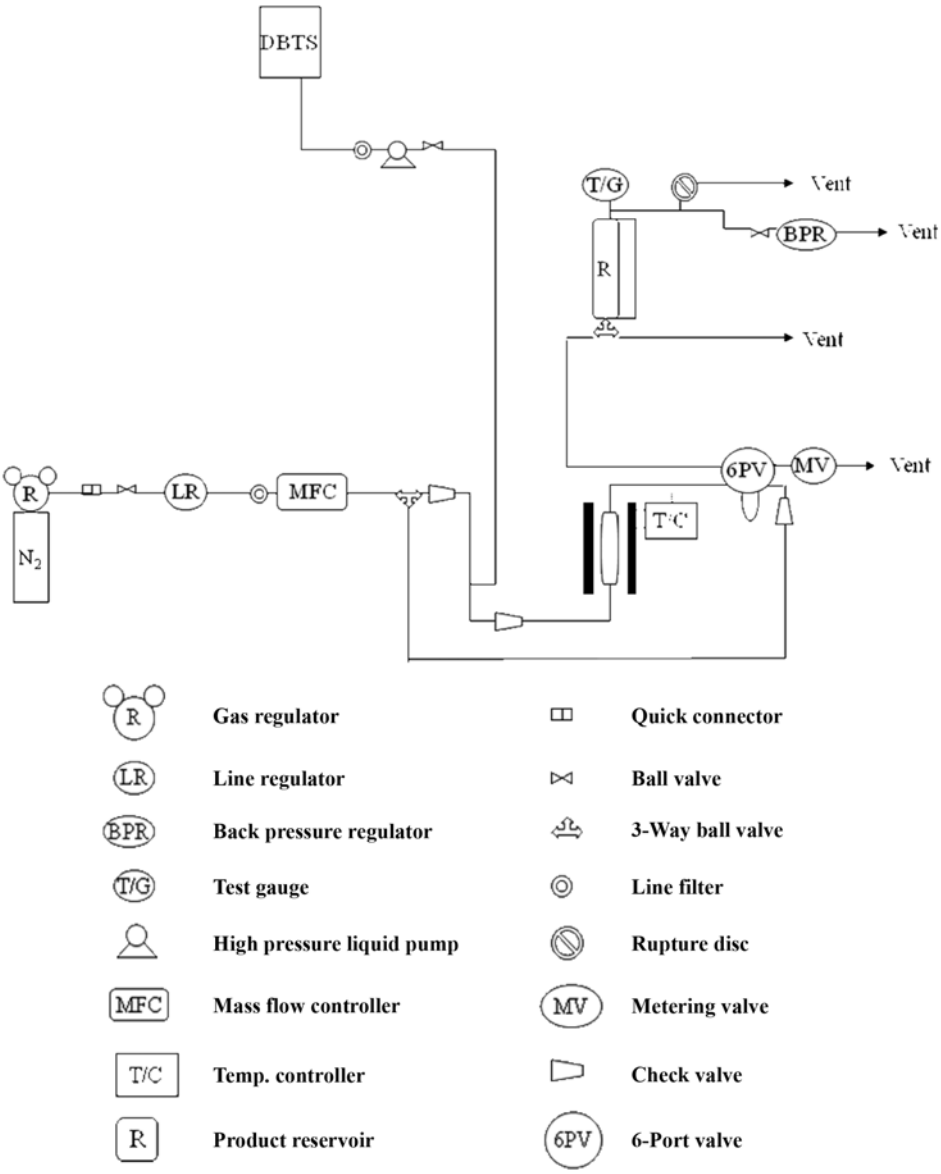

Fig. 1. Apparatus for DBTS decomposition.

Table 2. BET surface area and pore volume of catalysts synthesized by spray pyrolysis

Catalysts	BET surface area (m^2/g)	Pore volume (cm^3/g)[a]	Micropore volume (cm^3/g)[b]
MgAl	131	0.297	0.017
MgSiAl	149	0.420	0.011
MgSi	148	0.577	0.007

[a]BJH Desorption cumulative volume of pores between 1.7 nm and 300 nm diameter
[b]t-Plot micropore volume
[c]BJH Desorption average pore diameter (4V/A)

One of advantages of spray pyrolysis is to obtain fine and spherical particles [14-17]. Thus, we monitored the morphological changes of catalyst particles which were prepared by the spray pyrolysis. According to the SEM photos (Fig. 3(a) and (b)), the MgAl and the MgSiAl particles have no difference in overall particle shape. They are spherical and a mean size of about 0.7 μm. In the case of the MgSi sample as shown in Fig. 3(c), however, several hollow-and-fractured particles were found. The mean size of MgSi sample is about 0.9 μm, slightly larger than that of the MgAl and the MgSiAl. In a previous study, several hollow-and-fractured particles could be found during preparation of alumina particles through spray pyrolysis [15]. Such hollow particles support that the surface precipitation still occurs on the droplet during the drying step.

It was confirmed that no hexagonal ordered mesopore structure had formed because there was no clear peak under the 6° in small angle X-ray scattering (SAXS). An examination of the SAXS and nitrogen adsorption/desorption result showed that although the catalysts produced by spray pyrolysis had no ordered mesopore structure like materials in the M41S group, they were complex oxides with well-developed mesopores. Fig. 4 shows the XRD patterns of

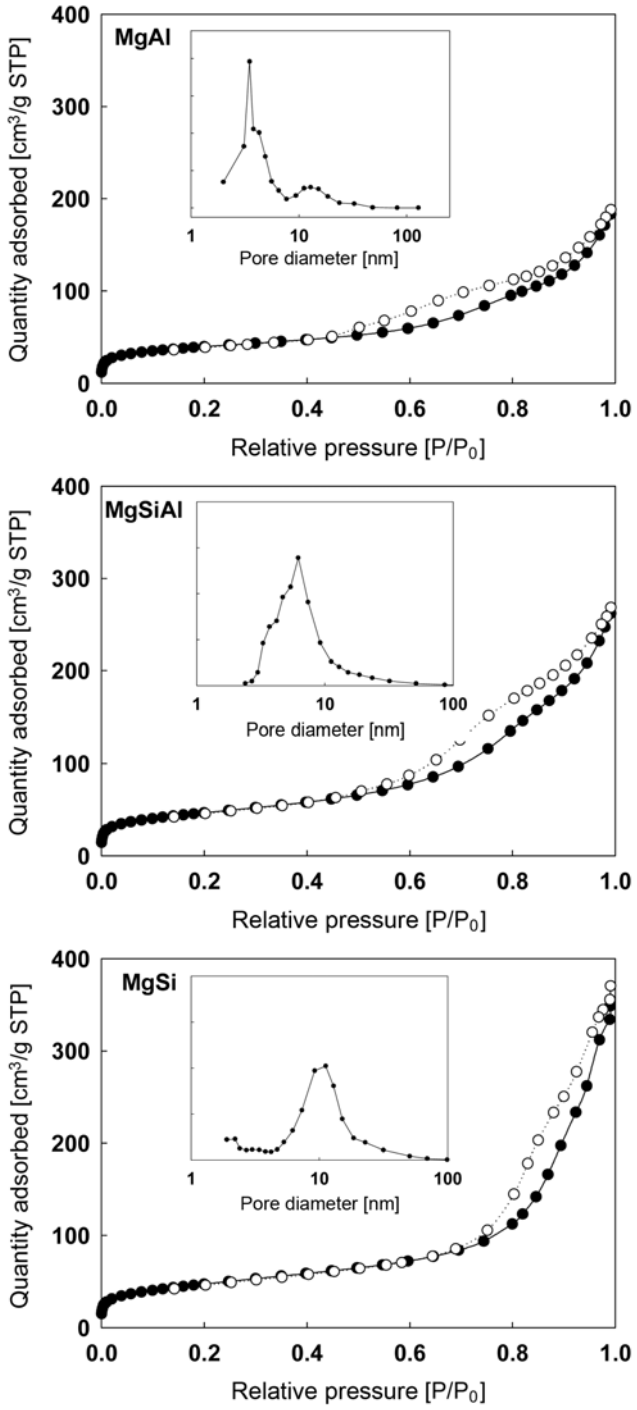

Fig. 2. Nitrogen adsorption/desorption isotherms and pore size distribution.

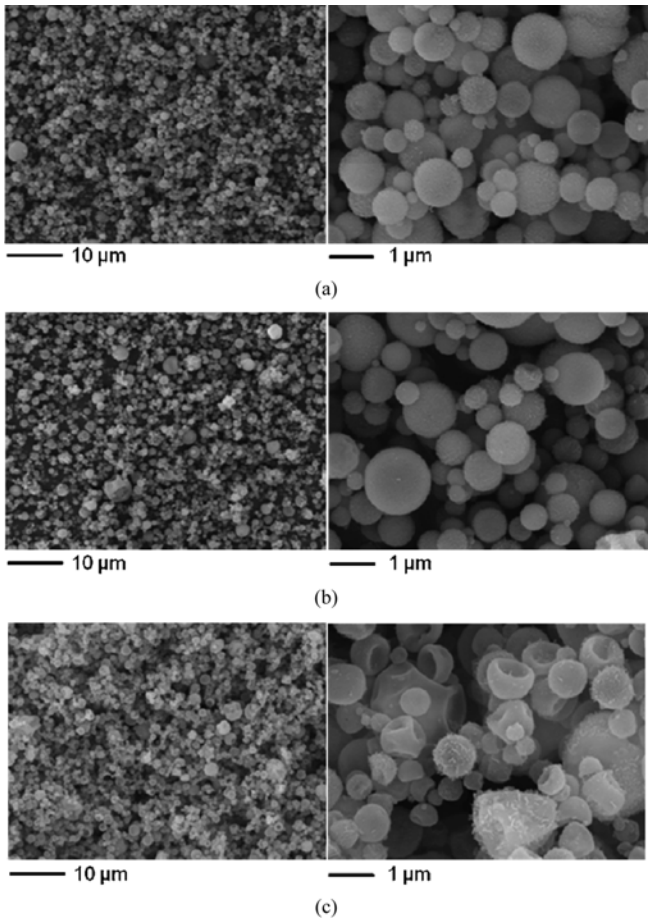

Fig. 3. SEM images of (a) MgAl, (b) MgSiAl, (c) MgSi.

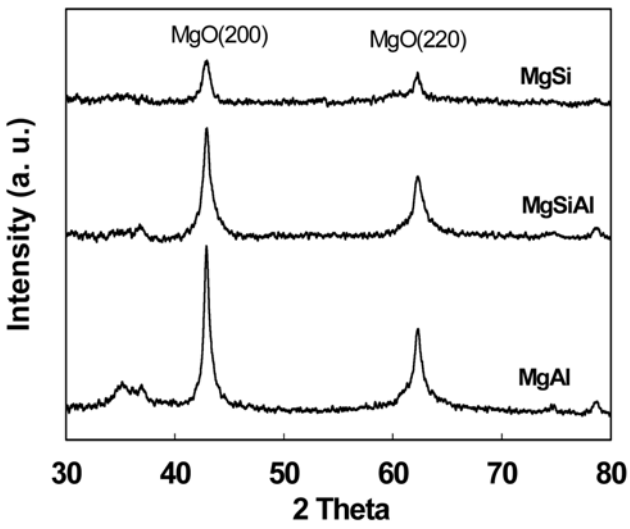

Fig. 4. X-ray diffraction patterns of different catalysts.

the catalysts. A comparison of the magnesium oxide peaks in the XRD patterns showed that the peak intensity was greater in MgAl followed in turn by MgSiAl and MgSi. This means that the MgSi catalyst has the smallest magnesium oxide particles, which were well dispersed.

The temperature-programmed desorption of carbon dioxide is used frequently to measure the number and strength of basic sites [25]. The strength and number of basic sites are reflected in the desorption temperature and peak area, respectively. The surface basicity of the catalysts was characterized by the temperature-programmed desorption of CO_2, and these profiles are presented in Fig. 5. In the MgO catalyst, which had a surface area of 29 m^2/g, a small and broad peak was observed at approximately 150 °C. This agrees with the finding of the maximum peak of the TPD plot of CO_2 desorbed from

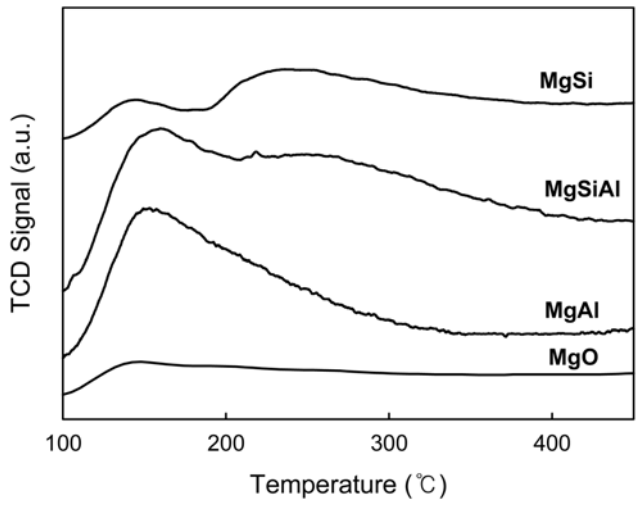

Fig. 5. CO_2-TPD profiles of the catalysts.

Table 3. Total basicity determined by CO_2-TPD of catalysts synthesized by spray pyrolysis

Catalysts	CO_2 consumption (mmol/g)
MgAl	2.43×10^{-2}
MgSiAl	3.22×10^{-2}
MgSi	2.94×10^{-2}

bulk MgO [22,23]. In the MgSiAl and MgSi catalysts, there were two distinct desorption peaks for each sample, indicating that there are two main types of basic sites. Although a peak of the CO_2-TPD plot desorbed from pure SiO_2 at approximately 100 ºC was reported [27], no such peak was observed in this study. This appears to be due to the very weak basicity of SiO_2 compared to MgO. The first peak at 150 ºC was assigned to the weak basic sites of bulk MgO, while the peaks at 270 ºC indicated the existence of strong basic sites resulting from the introduction of Mg^{2+} to the substrate [28]. Two different basic sites coexisted on the surface of the MgSiAl and MgSi catalysts. Table 3 lists the adsorbed CO_2 volume per gram of catalysts, which was calculated from the CO_2-TPD profiles and correlated with the basicity. The total amount of CO_2 desorbed from the MgSiAl catalyst was greater than that desorbed from the MgSi catalyst. As shown in Fig. 5, there were a larger number of weak basic sites than strong basic sites. On the other hand, the MgSi catalyst had a larger number of strong basic sites than weak basic sites. As a result, it was deduced that the basic sites on the MgSi catalyst were much stronger than those on the MgSiAl catalyst, even though the MgSiAl catalyst had a larger number of basic sites than the MgSi catalyst. This can be explained by the introduction of more Mg^{2+} into the MgSi framework, compared to MgAl and MgSiAl. This interpretation corresponds well to the result showing that the MgSi catalyst has a large surface area in nitrogen adsorption/desorption and that the MgSi catalyst shows the greatest dispersion of magnesium oxide, as shown in the XRD patterns.

2. Activity Measurements

DBTS decomposes to biphenyl and sulfur dioxide gas. Table 4 shows the conversion of the DBTS cracking reaction (time-on-stream of 6 hours). The conversion on the MgAl, MgSiAl, and MgSi catalysts were 53.1%, 68.9%, and 76.2%, respectively, which suggests that the MgSi catalyst has the highest activity. This can be attributed to the dispersed effect of the MgSi catalyst, which resulted in the significant exposure of basic sites. In addition, the basic sites over the MgSi catalyst were much stronger than those over the MgSiAl catalyst. This is in good agreement with a previous finding of base-catalytic reaction of DBTS cracking, in that the Mg-Al-mesoporous silica synthesized using a conventional self-assembly method in the liquid phase had higher catalytic performance than the pure MgO, further confirming that the basicity increased after being supported on mesoporous silica [24].

Table 4. DBTS conversion over different catalysts

Catalysts	DBTS conversion (%)
MgAl	53.1
MgSiAl	68.9
MgSi	76.2

Condition: 475 ºC, 100 psi, WHSV: 5 h^{-1}, Time-on-stream: 6 hr

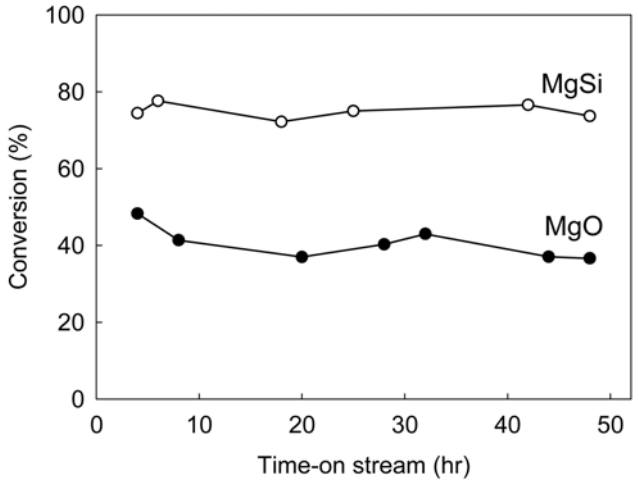

Fig. 6. Comparison of the time-on-stream stability of the MgSi catalyst with MgO catalyst. Reaction condition: 475 ºC, 100 psi, WHSV: 5 h^{-1}.

The MgSi catalyst was chosen for the long-term test, and the catalytic activity was compared with pure MgO. As shown in Fig. 6, the conversion of DBTS over the MgSi catalyst was always higher than that over the MgO catalyst. The level of DBTS conversion over the MgO catalyst was 48.3% after four hours of reaction, which began to decrease gradually after 32 hours reaching 36.7% after 48 hours. This suggests that the catalyst was deactivated. As for the MgSi catalyst, the DBTS conversion rate was 73.7% after 48 hours, which is considerably higher than that of MgO, and indicates that the catalyst was only slightly deactivated. The MgSi catalyst showed high activity and stability in the removal of sulfur dioxide from DBTS, which was attributed to the mesoporous structure and basic sites of the catalyst. More active sites could be exposed to the reactant owing to abundant pore channels and high surface area of the solid base facilitated, which means that MgSi has a better catalytic effect than the same amount of bulky MgO. Therefore, the MgSi solid base could improve the efficiency of the catalytic reactions remark-

ably. The strong basic sites resulted from the Mg^{2+} introduced into the SiO_2 lattice, and were anchored tightly to the substrate. Hence, the active sites of MgSi do not leach in the reaction, resulting in excellent stability.

CONCLUSIONS

MgSi catalyst synthesized by spray pyrolysis had well-developed mesopores and a large surface area. In addition, the magnesium oxide particles were well dispersed over the MgSi catalyst. According to CO_2 TPD results, the basic sites over the MgSi catalyst were much stronger than those over the MgSiAl and MgAl catalysts, even though the MgSiAl catalyst has a larger number of basic sites than the MgSi catalyst. The MgSi catalyst showed the highest activity in the decomposition of DBTS to biphenyl and sulfur dioxide gas. This was attributed to the dispersed effect of magnesium oxide over the MgSi catalyst, i.e., the basic sites well-dispersed on the catalyst are exposed and involved efficiently in the decomposition of DBTS. Compared to the MgO catalyst, the mesoporous MgSi catalyst synthesized by spray pyrolysis showed higher activity and stability in the removal of sulfur dioxide from DBTS, which may be due to the mesoporous structure and particular basic sites of the catalyst. Overall, the mesoporous MgSi solid base can improve the efficiency of the catalytic removal of sulfur dioxide from DBTS.

ACKNOWLEDGMENTS

The authors would like to acknowledge funding from the Korean Ministry of Knowledge Economy (MKE) through "Project of Energy & Resources Technology Development."

REFERENCES

1. A. Corma, *Chem. Rev.*, **97**, 2373 (1997).
2. G. V. R. Rao, G. P. Lopez, J. Bravo, H. Pham, A. K. Datye, H. Xu and T. L. Ward, *Adv. Mater.*, **14**, 1301 (2002).
3. R. I. Nooney, T. Dhanasekaran, Y. Chem, R. Josephs and A. E. Ostafin, *Chem. Mater.*, **14**, 4721 (2002).
4. J. S. Chung, D. J. Kim, W. S. Ahn, J. H. Ko and W. J. Cheong, *Korean J. Chem. Eng.*, **21**, 132 (2004).
5. H. S. Roh, J. S. Chang and S. E. Park, *Korean J. Chem. Eng.*, **16**, 331 (1999).
6. Y. Lu, H. Fan, A. Stump, T. L. Ward, T. Rieker and C. J. Brinker, *Nature*, **398**, 223 (1999).
7. T. B. Mangesh, B. R. Shailendra, L. W. Timothy and K. D. Abhaya, *Langmuir*, **19**, 256 (2003).
8. H. Fan, F. V. Swol, Y. Lu and C. J. Brinker, *J. Non-Crystal. Solids*, **258**, 71 (2001).
9. J. E. Hampsey, S. Arsenault, Q. Hu and Y. Lu, *Chem. Mater.,* **17**, 2475 (2005).
10. K. Y. Jung, Y. C. Kang and Y. K. Park, *J. Ind. Eng. Chem.*, **14**, 224 (2008).
11. K. Y. Jung and H. W. Lee, *J. Lumin*., **126**, 469 (2007).
12. A. Gurav, T. T. Kodas, T. Pluym and Y. Xiong, *Aerosol Sci. & Tech.*, **19**, 411 (1993).
13. J. Ortega and T. T. Kodas, *J. Aerosol Sci.*, **23**, 253 (1992).
14. C. M. Baek, K. Y. Jung, K. Y. Park, S. B. Park and S. B. Cho, *Korean Chem. Eng. Res.*, **46**, 880 (2008).
15. J. H. Kim, K. Y. Jung, K. Y. Park and S. B. Cho, *Micropor. Mesopor. Mater.*, In press (2009).
16. K. K. Lee, Y. C. Kang, K. Y. Jung and J. H. Kim, *J. Alloys Compd.*, **395**, 280 (2005).
17. D. S. Jung, S. K. Hong, H. J. Lee and Y. C. Kang, *J. Alloys Compd.*, **398**, 309 (2005).
18. A. Chica, A. Corma and M. E. Dómine, *J. Catal*., **242**, 299 (2006).
19. Y. Ono and T. Baba, *Catal. Today*, **38**, 321 (1997).
20. J. M. Hur, K. I. Park and H. I. Lee, *J. Korean Ind. Ing. Chem*., **11**, 563 (2000).
21. M. R. Kang, H. M. Lim, S. C. Lee, S. H. Lee and K. J. Kim, *J. Materials Online*, **6**, 218 (2004)
22. J. A. Kocal and T. A. Brandvold, US Patent 6,368,495 (2002).
23. G. Wu, X. Wang, N. Zhao, W. Wei and Y. Sun, Proc. 15th International Zeolite Conference, Beijing, 12-17 Aug., 1123 (2007).
24. N. You, M. J. Kim, K. E. Jeong, S. Y. Jeong, Y. K. Park and J. K. Jeon, *J. Nanosci. Nanotech.*, In press (2010).
25. H. Hattori, *Chem. Rev*., **95**, 537 (1995).
26. E. S. Umdu, M. Tuncer and E. Seker, *Bioresource Technol.*, **100**, 2828 (2009).
27. E. Seker, *International J. Hydrogen Energy*, **33**, 2044 (2008).
28. S. Liu, X. Zhang, J. Li, N. Zhao, W. Wei and Y. Sun, *Catal. Comm*., **9**, 1527 (2008).